

Motion Planning via Manifold Samples*

Oren Salzman¹, Michael Hemmer¹, Barak Raveh^{1,2}, and Dan Halperin¹

¹ Tel-Aviv University, Israel

² Hebrew University, Israel

Abstract. We present a general and modular algorithmic framework for path planning of robots. Our framework combines geometric methods for exact and complete analysis of low-dimensional configuration spaces, together with sampling-based approaches that are appropriate for higher dimensions. We suggest taking samples that are *entire low-dimensional manifolds of the configuration space*. These samples capture the connectivity of the configuration space much better than isolated point samples. Geometric algorithms then provide powerful primitive operations for complete analysis of the low-dimensional manifolds. We have implemented our framework for the concrete case of a polygonal robot translating and rotating amidst polygonal obstacles. To this end, we have developed a primitive operation for the analysis of an appropriate set of manifolds using arrangements of curves of rational functions. This modular integration of several carefully engineered components has led to a significant speedup over the PRM sampling-based algorithm, which represents an approach that is prevalent in practice.

1 Introduction

Motion planning is a fundamental research topic in robotics with applications in diverse domains such as graphical animation, surgical planning, computational biology and computer games. For a general overview of the subject and its applications see [1], [2], [3]. In its basic form, the motion-planning problem is to find a collision-free path for a robot or a moving object R in a *workspace* cluttered with static obstacles. The spatial pose of R , or the *configuration* of R , is uniquely defined by some set of parameters, the degrees of freedom (*dofs*) of R . The set of all robot configurations \mathcal{C} is termed the *configuration space* of the robot, and decomposes into the disjoint sets of free and forbidden configurations, which we denote by $\mathcal{C}_{\text{free}}$ and $\mathcal{C}_{\text{forb}}$, respectively. Thus, it is common to rephrase the motion-planning problem as the problem of moving R from a start configuration q_s to a target configuration q_t in a path that is fully contained within $\mathcal{C}_{\text{free}}$.

Analytic solutions to the general motion planning problem: The motion-planning problem is computationally hard with respect to the number of *dofs* [4],

* This work has been supported in part by the 7th Framework Programme for Research of the European Commission, under FET-Open grant number 255827 (CGL—Computational Geometry Learning), by the German-Israeli Foundation (grant no. 969/07), and by the Hermann Minkowski–Minerva Center for Geometry at Tel Aviv University.

yet much research has been devoted to solving the general problem and its various instances using geometric, algebraic and combinatorial tools. The configuration-space formalism was introduced by Lozano-Perez [5]. Schwartz and Sharir proposed the first general algorithm for solving the motion planning problem, with running time that is doubly-exponential in the number of *dofs* [6]. Singly exponential-time algorithms have followed [7], [8], [9], but are generally considered too complicated to be implemented in practice.

Solutions to low-dimensional instances of the problem: Although the general motion-planning problem cannot be efficiently solved analytically, more efficient algorithms have been proposed for various low-dimensional instances [2], such as translating a polygonal or polyhedral robot [10], [5], and translation with rotation of a polygonal robot in the plane [11], [12], [13]. For a survey of related approaches see [14]. Moreover, considerable advances in robust implementation of computational geometry algorithms in recent years have led to a set of implemented tools that are of interest in this context. Minkowski sums, which enable the representation of the configuration space of a translating robot, have robust and exact planar and 3-dimensional implementations [15], [16], [17].

Sampling-based approaches to motion planning: The sampling-based approach to motion-planning has extended the applicability of motion planning algorithms beyond the restricted subset of problems that can be solved efficiently by exact algorithms [1], [3]. Sampling-based motion planning algorithms, such as Probabilistic Roadmaps (PRM), Expansive Space Trees (EST) and Rapidly-exploring Random Trees (RRT) (see, e.g. [1, C.7], [3]) as well as their many variants, aim to capture the connectivity of $\mathcal{C}_{\text{free}}$ in a graph data structure, via random sampling of robot configurations. For a general survey on the field see [1]. Importantly, the PRM and RRT algorithms were both shown to be probabilistically complete [18], [19], [20], that is, they are guaranteed to find a valid solution, if one exists. However, the required running time for finding such a solution cannot be computed for new queries at run-time, and the proper usage of sampling-based approaches may still be considered somewhat of an art. Moreover, sampling-based methods are also considered sensitive to tight passages in the configuration space, due to the high-probability of missing such passages.

Hybrid methods for motion-planning: Few hybrid methods attempt to combine both deterministic and probabilistic planning strategies. Hirsch and Halperin [21] studied two-disc motion planning by exactly decomposing the configuration space of each robot, then combining the two solutions to a set of free, forbidden and mixed cells, and using PRM to construct the final connectivity graph. Zhang et al. [22] used PRM in conjunction with approximate cell decomposition, which also divides space into free, forbidden and mixed cells. Other studies have suggested to connect a dense set of near-by configuration space “slices”. Each slice is decomposed to free and forbidden cells, but adjacent slices are connected in an inexact manner, by e.g., identifying overlaps between adjacent slices [23, pp. 283-287], or heuristic interpolation and local-planning [24].

In [25] a 6 *dof* RRT planner is presented with a 3 *dof* local planner hybridizing probabilistic, heuristic and deterministic methods.

1.1 Contribution

In this study, we present a novel general scheme for motion planning via manifold samples (MMS), which extends sampling-based techniques like PRM as follows: Instead of sampling isolated robot configurations, we sample *entire low-dimensional manifolds*, which can be analyzed by complete and exact methods for decomposing space. This yields an explicit representation of maximal connected patches of free configurations on each manifold, and provides a much better coverage of the configuration space compared to isolated point samples. At the same time, the manifold samples are deliberately chosen such that they are likely to intersect each other, which allows to establish connections among different manifolds. The general scheme of MMS is illustrated in Figure 1. A detailed discussion of the scheme is presented in Section 2.

In Section 3, we discuss the application of MMS to the concrete case of a polygonal robot translating and rotating in the plane amidst polygonal obstacles. We present in detail appropriate families of manifolds as well as filtering schemes that should also be of interest for other scenarios. Although our software is prototypical, we emphasize that the achieved results are due to careful design and implementation on all levels. In particular, in Section 4 we present an exact analytic solution and efficient implementation to a motion planning problem instance: moving a polygonal robot in the plane with rotation and translation *along an arbitrary axis*. To the best of our knowledge the problem has not been analytically studied before. The implementation involves advanced algebraic and extension of state-of-the-art applied geometry tools. In Section 5 we present experimental results, which show our method’s superior behavior for several test cases vis-à-vis a common implementation of the sampling-based PRM algorithm. For example, in a tight passage scenario we demonstrate a 27-fold speedup in running time. We conclude with a discussion of extensions of our scheme, which we anticipate could greatly widen the scope of applicability of sampling-based methods for motion planning by combining them with strong analytic tools in a natural and straightforward manner.

2 General Scheme for Planning with Manifold Samples

Preprocessing—Constructing the connectivity graph: We propose a multi-query planner for motion planning problems in a possibly high-dimensional configuration space. The preprocessing stage constructs the *connectivity graph* of \mathcal{C} , a data structure that captures the connectivity of \mathcal{C} using manifolds as samples. The manifolds are decomposed into cells in $\mathcal{C}_{\text{free}}$ and $\mathcal{C}_{\text{forb}}$ in a complete and exact manner; we call a cell of the decomposed manifold that lies in $\mathcal{C}_{\text{free}}$ a *free space cell (FSC)* and refer to the connectivity graph as \mathcal{G} . The *FSCs* serve as nodes in \mathcal{G} while two nodes in \mathcal{G} are connected by an edge if their corresponding *FSCs* intersect. See Figure 1 for an illustration.

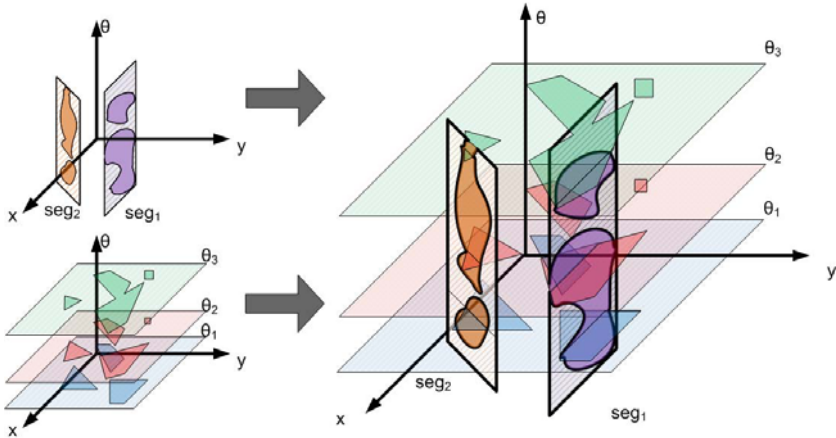


Fig. 1. Three-dimensional configuration space: The left side illustrates two families of manifolds where the decomposed cells are darkly shaded. The right side illustrates their intersection that induces the graph \mathcal{G} .

We formalize the preprocessing stage by considering manifolds induced by a family of constraints Ψ , such that $\psi \in \Psi$ defines a manifold m_ψ of the configuration space and FSC_{m_ψ} is the set of FSC s of m_ψ . The construction of a manifold m_ψ and its decomposition into FSC s are carried out via a Ψ -primitive, denoted P_Ψ , applied to an element $\psi \in \Psi$. By a slight abuse of notations we refer to an FSC both as a cell and as a node in the graph. Using this notation, Algorithm 1 summarizes the construction of \mathcal{G} . In lines 3-4, a new manifold constraint is generated and added to the collection X of manifold constraints. In lines 5-7, the manifold induced by the new constraint is decomposed by the appropriate primitive and its FSC s are added to \mathcal{G} .

Query: Once the connectivity graph \mathcal{G} has been constructed it can be queried for paths between two free configurations q_s and q_t in the following manner: A manifold that contains q_s (respectively q_t) in one of its FSC s is generated and

Algorithm 1. Construct Connectivity Graph

- 1: $V \leftarrow \emptyset, E \leftarrow \emptyset, X \leftarrow \emptyset$
 - 2: **repeat**
 - 3: $\psi \leftarrow \text{generate_constraint}(V, E, X)$
 - 4: $X \leftarrow X \cup \{\psi\}$
 - 5: $FSC_{m_\psi} \leftarrow P_\Psi(m_\psi)$
 - 6: $V \leftarrow V \cup \{\text{fsc} \mid \text{fsc} \in FSC_{m_\psi}\}$
 - 7: $E \leftarrow E \cup \{(\text{fsc}_1, \text{fsc}_2) \mid \text{fsc}_1 \in V, \text{fsc}_2 \in FSC_{m_\psi}, \text{fsc}_1 \cap \text{fsc}_2 \neq \emptyset \ \& \ \text{fsc}_1 \neq \text{fsc}_2\}$
 - 8: **until** stopping_condition
 - 9: **return** $G(V, E)$
-

decomposed. Its *FSCs* and their appropriate edges are added to \mathcal{G} . We compute a path γ in \mathcal{G} between the *FSCs* that contain q_s and q_t . A path in $\mathcal{C}_{\text{free}}$ may then be computed by planning a path within each *FSC* in γ .

2.1 Desirable Properties of Manifold Families

Choosing the specific set of manifold families may depend on the concrete problem at hand, as detailed in the next section. However, it seems desirable to retain some general properties. First, each manifold should be simple enough such that it is possible to decompose it into free and forbidden cells in a computationally efficient manner. The choice of manifold families should also *cover* the configuration space, such that each configuration intersects at least a single manifold m_ψ . In addition, local transitions between close-by configurations should be made possible via cross-connections of several intersecting manifolds, which we term the *spanning* property. We anticipate that these simple and intuitive properties (perhaps subject to some fine tuning) may lead to a proof of probabilistic completeness of the approach.

2.2 Exploration and Connection Strategies

A naïve way to generate constraints that induce manifolds is by random sampling. Primitives may be computationally complex and should thus be applied sparingly. We suggest a general exploration/connection scheme and additional optimization heuristics that may be used in concrete implementations of the proposed general scheme. We describe strategies in general terms, providing conceptual guidelines for concrete implementations, as demonstrated in Section 3.

Exploration and connection phases: Generation of constraints is done in two phases: *exploration* and *connection*. In the exploration phase constraints are generated such that primitives will produce *FSCs* that introduce new connected components in $\mathcal{C}_{\text{free}}$. The aim of the exploration phase is to increase the coverage of the configuration space as efficiently as possible. In contrast, in the connection phase constraints are generated such that primitives will produce *FSCs* that connect existing connected components in \mathcal{G} . Once a constraint is generated, \mathcal{G} is updated as described above. Finally, we note that we can alternate between exploration and connection, namely we can decide to further explore after some connection work has been performed.

Region of interest (RoI): Decomposing an entire manifold m_ψ by a primitive P_ψ may be unnecessary. Patches of m_ψ may intersect $\mathcal{C}_{\text{free}}$ in highly explored parts or connect already well-connected parts of \mathcal{G} while others may intersect $\mathcal{C}_{\text{free}}$ in sparsely explored areas or less well connected parts of \mathcal{G} . Identifying the regions where the manifold is of good use (depending on the phase) and constructing m_ψ only in those regions increases the effectiveness of P_ψ while desirably biasing the samples. We refer to a manifold patch that is relevant in a specific phase as the *Region of Interest* - RoI of the manifold.

Constraint filtering: Let $\psi \in \Psi$ be a constraint such that applying P_ψ to ψ yields the set of *FSCs* on m_ψ . If we are in the *connection* phase, inserting the

associated nodes into \mathcal{G} and intersecting them with the existing *FSC*s should connect existing connected components of \mathcal{G} . Otherwise, the primitive’s contribution is poor. We suggest applying a filtering predicate immediately after generating a constraint ψ to check if $P_\psi(\psi)$ may connect existing connected components of \mathcal{G} . If not, m_ψ should not be constructed and ψ should be discarded.

3 The Case of Rigid Polygonal Motion

We demonstrate the scheme suggested in Section 2 by considering a (not necessarily convex) polygonal robot R translating and rotating in the plane amidst polygonal obstacles. A configuration of R describes the position of the reference point (chosen arbitrarily) of R and the orientation of R . As we consider full rotations, the configuration space \mathcal{C} is the three dimensional space $\mathbb{R}^2 \times S^1$.

3.1 Manifold Families

As defined in Section 2, we consider manifolds defined by *constraints* and construct and decompose them using *primitives*. We suggest the following constraints restricting motions of the robot R and describe their associated primitives: (i) The **Angle Constraint** fixes the orientation of R while it is still free to translate anywhere within the workspace, and (ii) the **Segment Constraint** restricts the position of the reference point to a segment in the workspace while R is free to rotate.

The left part of Figure 1 demonstrates decomposed manifolds associated to the angle (left bottom) and segment (left top) constraints. The angle constraint induces a two-dimensional horizontal plane where the cells are polygons. The segment constraint induces a two-dimensional vertical slab where the cells are defined by the intersection of rational curves (as explained in Section 4).

We delay the discussion of creating and decomposing manifolds to Section 4. For now, notice that the Segment-Primitive is computationally far more time-consuming than the Angle-Primitive, since it involves arrangements¹ of curves of higher algebraic degree.

3.2 Exploration and Connection Strategies

We use manifolds constructed by the Angle-Primitive for the exploration phase and manifolds constructed by the Segment-Primitive for the connection phase. Since the Segment-Primitive is far more costly than the Angle-Primitive, we focused our efforts on optimizing the former.

Region of interest - RoI: As suggested in Section 2.2 we may consider the Segment-Primitive in a subset of the range of angles. This results in a somewhat “weaker” yet more efficient primitive than considering the whole range. If the connectivity of a local area of the configuration space is desired, then using this optimization may suffice while considerably speeding up the algorithm.

Generating segments: Let fsc be a random *FSC*. Consecutive layers (manifolds of the Angle Constraint) have a similar structure unless topological criticalities

¹ A subdivision of the plane into zero-dimensional, one-dimensional and two-dimensional cells, called vertices, edges and faces, respectively induced by the curves.

occur in \mathcal{C} . Once such a criticality occurs, an *FSC* either appears and grows or shrinks and disappears. We thus suggest a heuristic for generating a segment in the workspace for the Segment-Primitive using the size of *fsc* as a parameter where we refer to small and large cells according to pre-defined constants. The RoI used will be proportional to the size of *fsc*. The segment generated will be chosen with one of the following procedures used in Algorithm 2:

Algorithm 2. Generate Segment Constraint (V, E)

```

1:  $r \leftarrow \text{random\_num}([0, 1])$ 
2: if  $r \geq \text{random\_threshold}$  then
3:   return  $\text{random\_segment\_procedure}()$ 
4: else
5:    $\text{fsc} \leftarrow \text{random\_fsc}(V)$ 
6:    $\alpha \leftarrow [\text{size}(\text{fsc}) - \text{small\_cell\_size}] / [\text{large\_cell\_size} - \text{small\_cell\_size}]$ 
7:   if  $r \geq \alpha$  then
8:     return  $\text{small\_cell\_procedure}(\text{fsc}, V)$ 
9:   else
10:    return  $\text{large\_cell\_procedure}(\text{fsc}, V)$ 
11:  end if
12: end if

```

Algorithm 3. Filter Segment (s, RoI, V, E)

```

1:  $cc_{ids} \leftarrow \emptyset$ 
2: for all  $v \in V$  do
3:    $\text{fsc} \leftarrow \text{free\_space\_cell}(v)$ 
4:   if  $\text{constraining\_angle}(\text{fsc}) \in \text{RoI}$  then
5:      $cc_{ids} \leftarrow cc_{ids} \cup \text{connected\_component\_id}(v)$ 
6:   end if
7: end for
8: if  $|cc_{ids}| \leq 1$  then
9:   return  $\text{filter\_out}$ 
10: end if

```

(i) **Random procedure:** Return a random segment from the workspace. (ii) **Large cell procedure:** Return a random segment from the projection of *fsc* onto the xy -plane. (iii) **Small cell procedure:** Return a segment by considering *fsc* and an adjacent layer. For full details see [26].

Constraint Filtering: As suggested in Section 2.2, we avoid computing unnecessary primitives. All *FSCs* that will intersect a “candidate” constraint s , namely all *FSCs* of layers in its RoI, are tested. If they are all in the same connected component in \mathcal{G} , s can be discarded as demonstrated in Algorithm 3.

3.3 Path Planning Query

A configuration q is marked by (x, y, θ) where x, y is the location of the reference point and θ is the amount of counterclockwise rotation of R relative to its original placement. For a query $q = (q_1, q_2)$, where $q_i = (x_i, y_i, \theta_i)$, $i \in 1, 2$, m_{θ_1} and m_{θ_2}

are constructed and $FSC_{m_{\theta_1}}, FSC_{m_{\theta_2}}$ are added to \mathcal{G} . A path of FSC s between the FSC s containing q_1 and q_2 is searched for. A local path in an Angle-Primitive's FSC (which is a polygon) is constructed by computing the shortest path on the visibility graph defined inside the polygon by the vertices of the polygon. A local path in an FSC of a Segment-Primitive (which is a two-dimensional region bounded by rational arcs) is constructed by applying cell decomposition and computing the shortest path on the graph induced by the decomposed cells.

4 Efficient Implementation of Manifold Decomposition

The algorithm discussed in Section 3 is implemented in C++. It is based on CGAL's arrangement package, which is used for the geometric primitives, and the BOOST graph library [27], which is used to represent the connectivity graph \mathcal{G} . We next discuss the manifold decomposition methods in more detail.

Angle-Primitive: The Angle-Primitive for a constraining angle θ (denoted $P_{\theta}(\theta)$) is constructed by computing the Minkowski sum of $-R_{\theta}$ with the obstacles². The implementation is an application of CGAL's Minkowski sums package [28, C.24]. We remark that we ensure (using the method of Canny et al. [29]) that the angle θ is chosen such that $\sin \theta$ and $\cos \theta$ are rational. This allows for an exact rotation of the robot and an exact computation of the Minkowski Sum.

Segment-Primitive: Limiting the possible positions of the robot's reference point r to a given segment s , results in a two-dimensional configuration space. Each vertex (or edge) of the robot in combination with each edge (or vertex) of an obstacle gives rise to a critical curve in this configuration space. Namely the set of all configurations that put the two features into contact, and thus mark a potential transition between $\mathcal{C}_{\text{forb}}$ and $\mathcal{C}_{\text{free}}$. Our analysis [26] shows that these critical curves can be expressed by rational functions only. Thus, the implementation of the Segment-Primitive is first of all a computation of an arrangement of rational functions.

CGAL follows the *generic programming paradigm* [30], that is, algorithms are formulated and implemented such that they abstract away from the actual types, constructions and predicates. Using the C++ programming language this is realized by means of class and function templates. In particular, the arrangement package is written such that it takes a traits class as a template argument. This traits class defines the supported curve type and provides the operations that are required for this type. Since the old specialized traits class was too slow for MMS to be effective (even slower than the solution for general algebraic curves presented in [31]), we devised a new efficient traits class for rational functions.

The new traits class [26] is written such that it takes maximal advantage of the fact that the supported curves are functions. As opposed to the general traits in [31], we never have to shear the coordinate system and we only require tools provided by the univariate algebraic kernel of CGAL [28, C.8]. A comparison using the benchmark instances that were also used in [31] shows that the new

² We use $-R_{\theta}$ to denote R rotated by θ and reflected about the origin.

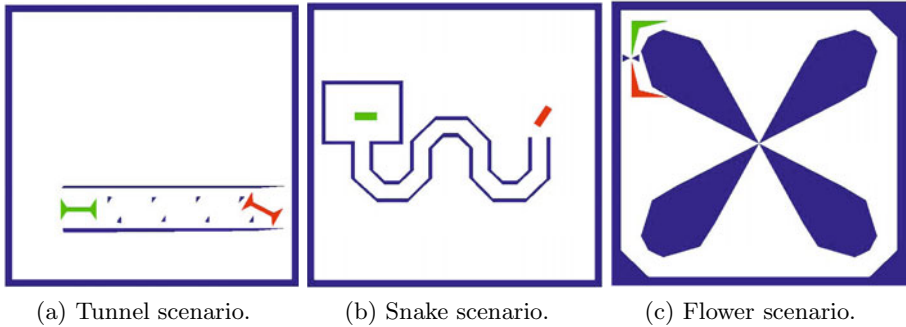


Fig. 2. Experimental scenarios

traits class is about 3-4 times faster than the general traits class; this is a total speed up of about 10 when compared to the old dedicated traits class.

The development of this new traits class represents the low tier of our efforts to produce an effective motion planner and relies on a more intimate acquaintance with CGAL in general and the arrangement traits for algebraic curves in particular; for further details see [26]. We note that the new traits class has been integrated into CGAL and will be available in the upcoming CGAL release 3.9.

5 Experimental Results

We demonstrate the performance of our planner using three different scenarios. All scenarios consist of a workspace, a robot with obstacles and one query (source and target configurations). Figure 2 illustrates the scenarios where the obstacles are drawn in blue and the source and target configurations are drawn in green and red, respectively. All reported tests were measured on a Dell 1440 with one 2.4GHz P8600 Intel Core 2 Duo CPU processor and 3GB of memory running with a Windows 7 32-bit OS. Preprocessing times presented (in seconds) are times that yielded at least 80% (minimum of 5 runs) success rate in solving queries.

5.1 Algorithm Properties

Our planner has two parameters: the number n_θ of layers to be generated and the number n_s of segment constraints to be generated. We chose the following values for these parameters: $n_\theta \in \{10, 20, 40, 80\}$ and $n_s \in \{2^i | i \in \mathbb{N}, i \leq 14\}$. For a pair of parameters (n_θ, n_s) we report the preprocessing time t and whether a path was found (marked \checkmark) or not (marked \times) once the query was issued. The results for the flower scenario are reported in Table 1. We show that a considerable increase in parameters has only a limited effect on the preprocessing time.

In order to test the effectiveness of our optimizations, we ran the planner with or without any heuristic for choosing segments and with or without segment filtering. We also added a test with all optimizations using the old traits class. The results for the flower scenario can be viewed in Table 2. We remark that the

Table 1. Parameter sensitivity

| | | n_θ | | | |
|-------|------|------------|--------|--------|--------|
| | | 10 | 20 | 40 | 80 |
| n_s | 256 | (6,×) | (11,×) | (12,×) | (16,×) |
| | 512 | (7,×) | (13,×) | (14,×) | (25,×) |
| | 1024 | (16,×) | (20,✓) | (23,✓) | (35,✓) |
| | 2048 | (30,×) | (35,✓) | (38,✓) | (51,✓) |
| | 4096 | (46,✓) | (53,✓) | (60,✓) | (82,✓) |

Table 2. Optimization results

| Traits | Segment Generation | Filtering | n_θ | n_s | t |
|--------|--------------------|-----------|------------|-------|------|
| New | random | not used | 20 | 8192 | 1418 |
| | | used | 20 | 8192 | 112 |
| | heuristic | not used | 40 | 512 | 103 |
| | | used | 20 | 1024 | 20 |
| Old | heuristic | used | 20 | 1024 | 138 |

engineering work invested in optimizing MMS yielded an algorithm comparable and even surpassing a motion planner that is in prevalent use as shown next.

5.2 Comparison with PRM

We used an implementation of the PRM algorithm as provided by the OOPSMP package [32]. For fair comparison, we did not use cycles in the roadmap as cycles increase the preprocessing time significantly. We manually optimized the parameters of each planner over a concrete set. As with previous tests, the parameters for MMS are n_θ and n_s . The parameters used for the PRM are the number of neighbors (denoted k) to which each milestone should be connected and the percentage of time used to sample new milestones (denoted % st in Table 3).

Furthermore, we ran the flower scenario several times, progressively increasing the robot size. This caused a “tightening” of the passages containing the desired path. Figure 3 demonstrates the preprocessing time as a function of the tightness of the problem for both planners. A tightness of zero denotes the base scenario (Figure 2c) while a tightness of one denotes the tightest problem solved.

The results show a speedup for all scenarios when compared to the PRM implementation. Moreover, our algorithm has little sensitivity to the tightness of the problem as opposed to the PRM algorithm. In the tightest experiment, MMS runs 27 times faster than the PRM implementation.

6 Further Directions

To conclude, we outline directions for extending and enhancing the current work. Our primary goal is to use the MMS framework to solve progressively more com-

Table 3. Comparison with PRM

| Scenario | MMS | | | PRM | | | Speedup |
|----------|------------|-------|-----|-----|--------|-----|---------|
| | n_θ | n_s | t | k | % st | t | |
| Tunnel | 20 | 512 | 100 | 20 | 0.0125 | 180 | 1.8 |
| Snake | 40 | 256 | 22 | 20 | 0.025 | 140 | 6.3 |
| Flower | 20 | 1024 | 20 | 24 | 0.0125 | 40 | 2 |

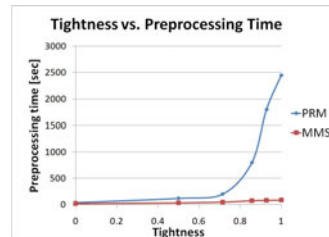


Fig. 3. Tightness results

plicated motion-planning problems. As suggested earlier, we see the framework as a platform for convenient transfer of strong geometric primitives into motion planning algorithms. For example, among the recently developed tools are efficient and exact solutions for computing the Minkowski sums of polytopes in \mathbb{R}^3 (see Introduction) as well as for exact update of the sum when the polytopes rotate [33]. These could be combined into an MMS for planning full rigid motion of a polytope among polytopes, which, extrapolating from the current experiments could outperform more simplistic solutions in existence.

Looking at more intricate problems, we anticipate some difficulty in turning constraints into manifolds that can be exactly decomposed. We propose to have manifolds where the decomposition yields some *approximation* of the *FSCs*, using recent advanced meshing tools for example. We can endow the connectivity-graph nodes with an attribute describing their approximation quality. One can then decide to only look for paths all whose nodes are above a certain approximation quality. Alternatively, one can extract any solution path and then refine only those portions of the path that are below a certain quality.

Beyond motion planning: We foresee an extension of the framework to other problems that involve high-dimensional arrangements of critical hypersurfaces. It is difficult to describe the entire arrangement analytically, but there are often situations where constraint manifolds could be computed analytically. Hence, it is possible to shed light on problems such as loop closure and assembly planning where we can use manifold samples to analytically capture pertinent information of high-dimensional arrangements of hypersurfaces. Notice that although in Section 3 we used only planar manifolds, there are recently developed tools to construct two-dimensional arrangement of curves on curved surfaces [34] which gives further flexibility in choosing the manifold families.

For supplementary material and updates the reader is referred to our webpage <http://acg.cs.tau.ac.il/projects/mms>.

References

1. Choset, H., Burgard, W., Hutchinson, S., Kantor, G., Kavvaki, L.E., Lynch, K., Thrun, S.: Principles of Robot Motion: Theory, Algorithms, and Implementation. MIT Press, Cambridge (2005)
2. Latombe, J.C.: Robot Motion Planning. Kluwer Academic Publishers, Norwell (1991)
3. LaValle, S.M.: Planning Algorithms. Cambridge University Press, Cambridge (2006)
4. Reif, J.H.: Complexity of the mover's problem and generalizations. In: FOCS, pp. 421–427. IEEE Computer Society, Washington, DC, USA (1979)
5. Lozano-Perez, T.: Spatial planning: A configuration space approach. MIT AI Memo 605 (1980)
6. Schwartz, J.T., Sharir, M.: On the “piano movers” problem: II. General techniques for computing topological properties of real algebraic manifolds. Advances in Applied Mathematics 4(3), 298–351 (1983)

7. Basu, S., Pollack, R., Roy, M.F.: Algorithms in Real Algebraic Geometry. Algorithms and Computation in Mathematics. Springer, Heidelberg (2003)
8. Canny, J.F.: Complexity of Robot Motion Planning (ACM Doctoral Dissertation Award). MIT Press, Cambridge (1988)
9. Chazelle, B., Edelsbrunner, H., Guibas, L.J., Sharir, M.: A singly exponential stratification scheme for real semi-algebraic varieties and its applications. *Theoretical Computer Science* 84(1), 77–105 (1991)
10. Aronov, B., Sharir, M.: On translational motion planning of a convex polyhedron in 3-space. *SIAM J. Comput.* 26(6), 1785–1803 (1997)
11. Avnaim, F., Boissonnat, J., Faverjon, B.: A practical exact motion planning algorithm for polygonal object amidst polygonal obstacles. In: Boissonnat, J.-D., Laumond, J.-P. (eds.) *Geometry and Robotics*. LNCS, vol. 391, pp. 67–86. Springer, Heidelberg (1989)
12. Halperin, D., Sharir, M.: A near-quadratic algorithm for planning the motion of a polygon in a polygonal environment. *Disc. Comput. Geom.* 16(2), 121–134 (1996)
13. Schwartz, J.T., Sharir, M.: On the “piano movers” problem: I. The case of a two-dimensional rigid polygonal body moving amidst polygonal barriers. *Commun. Pure appl. Math.* 35, 345–398 (1983)
14. Sharir, M.: Algorithmic Motion Planning. In: *Handbook of Discrete and Computational Geometry*, 2nd edn., CRC Press, Inc., Boca Raton (2004)
15. Fogel, E., Halperin, D.: Exact and efficient construction of Minkowski sums of convex polyhedra with applications. *CAD* 39(11), 929–940 (2007)
16. Hachenberger, P.: Exact Minkowski sums of polyhedra and exact and efficient decomposition of polyhedra into convex pieces. *Algorithmica* 55(2), 329–345 (2009)
17. Wein, R.: Exact and efficient construction of planar minkowski sums using the convolution method. In: Azar, Y., Erlebach, T. (eds.) *ESA 2006*. LNCS, vol. 4168, pp. 829–840. Springer, Heidelberg (2006)
18. Kavvaki, L.E., Kolountzakis, M.N., Latombe, J.C.: Analysis of probabilistic roadmaps for path planning. *IEEE Trans. Robot. Automat.* 14(1), 166–171 (1998)
19. Kuffner, J.J., Lavalle, S.M.: RRT-Connect: An efficient approach to single-query path planning. In: *ICRA*, pp. 995–1001. IEEE, Los Alamitos (2000)
20. Ladd, A.M., Kavvaki, L.E.: Generalizing the analysis of PRM. In: *ICRA*, pp. 2120–2125. IEEE, Los Alamitos (2002)
21. Hirsch, S., Halperin, D.: Hybrid motion planning: Coordinating two discs moving among polygonal obstacles in the plane. In: *WAFR 2002*, pp. 225–241 (2002)
22. Zhang, L., Kim, Y.J., Manocha, D.: A hybrid approach for complete motion planning. In: *IROS*, pp. 7–14 (2007)
23. De Berg, M., Cheong, O., van Kreveld, M., Overmars, M.: *Computational Geometry: Algorithms and Applications*. Springer, Heidelberg (2008)
24. Lien, J.M.: Hybrid motion planning using Minkowski sums. In: *RSS 2008* (2008)
25. Yang, J., Sacks, E.: RRT path planner with 3 DOF local planner. In: *ICRA*, pp. 145–149. IEEE, Los Alamitos (2006)
26. Salzman, O., Hemmer, M., Raveh, B., Halperin, D.: Motion planning via manifold samples. In: *arXiv:1107.0803* (2011)
27. Siek, J.G., Lee, L.-Q., Lumsdaine, A.: *The Boost Graph Library: User Guide and Reference Manual*. Addison-Wesley Professional, Reading (2001)
28. The CGAL Project: *CGAL User and Reference Manual*. 3.7 edn. CGAL Editorial Board (2010), <http://www.cgal.org/>

29. Canny, J., Donald, B., Ressler, E.K.: A rational rotation method for robust geometric algorithms. In: SoCG 1992, pp. 251–260. ACM, New York (1992)
30. Austern, M.H.: *Generic Programming and the STL*. Addison-Wesley, Reading (1998)
31. Berberich, E., Hemmer, M., Kerber, M.: A generic algebraic kernel for non-linear geometric applications. In: SoCG 2011 (2011)
32. Plaku, E., Bekris, K.E., Kavraki, L.E.: OOPS for motion planning: An online open-source programming system. In: ICRA, pp. 3711–3716. IEEE, Los Alamitos (April 2007)
33. Mayer, N., Fogel, E., Halperin, D.: Fast and robust retrieval of Minkowski sums of rotating convex polyhedra in 3-space. In: SPM, pp. 1–10 (2010)
34. Berberich, E., Fogel, E., Halperin, D., Mehlhorn, K., Wein, R.: Arrangements on parametric surfaces I: General framework and infrastructure. *Mathematics in Computer Science* 4(1), 45–66 (2010)